SYSTEMS BIOLOGY

The regulatory enzymes and protein substrates for the lysine β-hydroxybutyrylation pathway

He Huang[1,2*†], Di Zhang[3*], Yejing Weng[3], Kyle Delaney[3], Zhanyun Tang[4], Cong Yan[1,2], Shankang Qi[1,2], Chao Peng[3‡], Philip A. Cole[5], Robert G. Roeder[4], Yingming Zhao[3†]

Metabolism-mediated epigenetic changes represent an adapted mechanism for cellular signaling, in which lysine acetylation and methylation have been the historical focus of interest. We recently discovered a β-hydroxybutyrate–mediated epigenetic pathway that couples metabolism to gene expression. However, its regulatory enzymes and substrate proteins remain unknown, hindering its functional study. Here, we report that the acyltransferase p300 can catalyze the enzymatic addition of β-hydroxybutyrate to lysine (Kbhb), while histone deacetylase 1 (HDAC1) and HDAC2 enzymatically remove Kbhb. We demonstrate that p300-dependent histone Kbhb can directly mediate in vitro transcription. Moreover, a comprehensive analysis of Kbhb substrates in mammalian cells has identified 3248 Kbhb sites on 1397 substrate proteins. The dependence of histone Kbhb on p300 argues that enzyme-catalyzed acylation is the major mechanism for nuclear Kbhb. Our study thus reveals key regulatory elements for the Kbhb pathway, laying a foundation for studying its roles in diverse cellular processes.

INTRODUCTION

In addition to serving as an energy source and metabolic intermediate, a metabolite can exert a signaling function by binding to a protein either covalently or noncovalently. Covalent binding to proteins occurs either through spontaneous chemical reactions (*1*, *2*) or enzyme-catalyzed reactions (*3*, *4*). As examples, acetyl coenzyme A (CoA) and *S*-adenosylmethionine can be used by acetyltransferases and methyltransferases for lysine acetylation (Kac) and methylation, respectively (*3*, *5*). While many metabolites' roles in metabolism are largely known, their functions in cellular signaling and regulation remain to be explored.

Ketone bodies, including acetone, acetoacetate, and β-hydroxybutyrate, are products of lipid metabolism. Liver-produced ketone bodies can serve as an alternative energy source to glucose for peripheral tissues that include the brain (*6*). The concentration of β-hydroxybutyrate in blood can be dynamically regulated under some physiopathological conditions. For example, it can be elevated from 0.1 mM or lower to 2 to 3.8 mM during starvation (*7*), intense exercise (*8*), and diabetic ketoacidosis (*9*). β-Hydroxybutyrate is the key element of ketogenic diet and has been used as a drug for epilepsy (*10*). In addition, this compound has been investigated for its possible use as an adjuvant for cancer therapeutics (*11*). These lines of evidence suggest that β-hydroxybutyrate has functions beyond serving as an energy source.

Our recent work indicates that β-hydroxybutyrate is a precursor for a type of previously unknown posttranslational modification (PTM), lysine β-hydroxybutyrylation (Kbhb) (*12*). We identified 36 Kbhb marks on histones. This type of histone mark is markedly induced in response to the concentration of β-hydroxybutyrate during starvation and in mouse models of type I diabetes. Histone Kbhb plays important roles in gene expression. For example, H3K9bhb is associated with active gene expression of multiple metabolic pathways in response to starvation. Therefore, our results indicated that histone Kbhb is a type of previously unknown PTM that is physiologically relevant and can contribute to transcription regulation. Despite these findings, key regulatory elements of Kbhb pathway, including "writers," "erasers," and "readers," and protein substrates bearing this modification, remain largely unknown, thereby hindering its biological characterization.

Here, we biochemically characterized the Kbhb pathway using biochemical and proteomic approaches. Beyond a proof-of-principle demonstration of a direct function of Kbhb in transcription, we identified writer and eraser proteins for this PTM. We carried out a proteomic screen, identifying 3248 unique Kbhb sites on 1397 proteins in human embryonic kidney (HEK) 293 cells. Together, this study validates the regulation of Kbhb by pharmacologically targetable enzymes, expands the list of protein substrates and pathways potentially regulated by Kbhb, and lays the foundation necessary for further interrogation of the roles of Kbhb in various physiopathological conditions.

RESULTS

p300 catalyzes histone Kbhb and stimulates transcription in vitro

Our earlier study suggested that histone H3K9bhb is a dynamic and active histone mark during starvation (*12*). We therefore hypothesized that Kbhb is a type of reversible PTM that can be regulated by enzymes with opposite activities, in a fashion similar to that for Kac (Fig. 1A). p300 has been identified as an acyltransferase for acetylation, propionylation, and crotonylation (*3*). Further biophysical studies showed that the ac-CoA–binding pocket of p300 can preferentially accommodate uncharged short-chain acyl-CoAs (*13*). Thus, it is highly likely that p300 can catalyze Kbhb reaction.

To gain further support for Kbhb function, we took advantage of an in vitro–reconstituted transcription system that involves the

[1]Shanghai Institute of Materia Medica, Chinese Academy of Sciences, Shanghai 201203, China. [2]University of Chinese Academy of Sciences, Beijing 100049, China. [3]Ben May Department for Cancer Research, The University of Chicago, Chicago, IL 60637, USA. [4]Laboratory of Biochemistry and Molecular Biology, The Rockefeller University, New York, NY 10065, USA. [5]Division of Genetics, Department of Medicine, Brigham and Women's Hospital, Department of Biological Chemistry and Molecular Pharmacology, Harvard Medical School, Boston, MA 02115, USA.
*These authors contributed equally to this work.
†Corresponding author. Email: yingming.zhao@uchicago.edu (Y.Z.); hhuang@simm.ac.cn (H.H.)
‡Present address: National Facility for Protein Science in Shanghai, Zhangjiang Lab, Shanghai Advanced Research Institute, Chinese Academy of Sciences, Shanghai 201210, China.

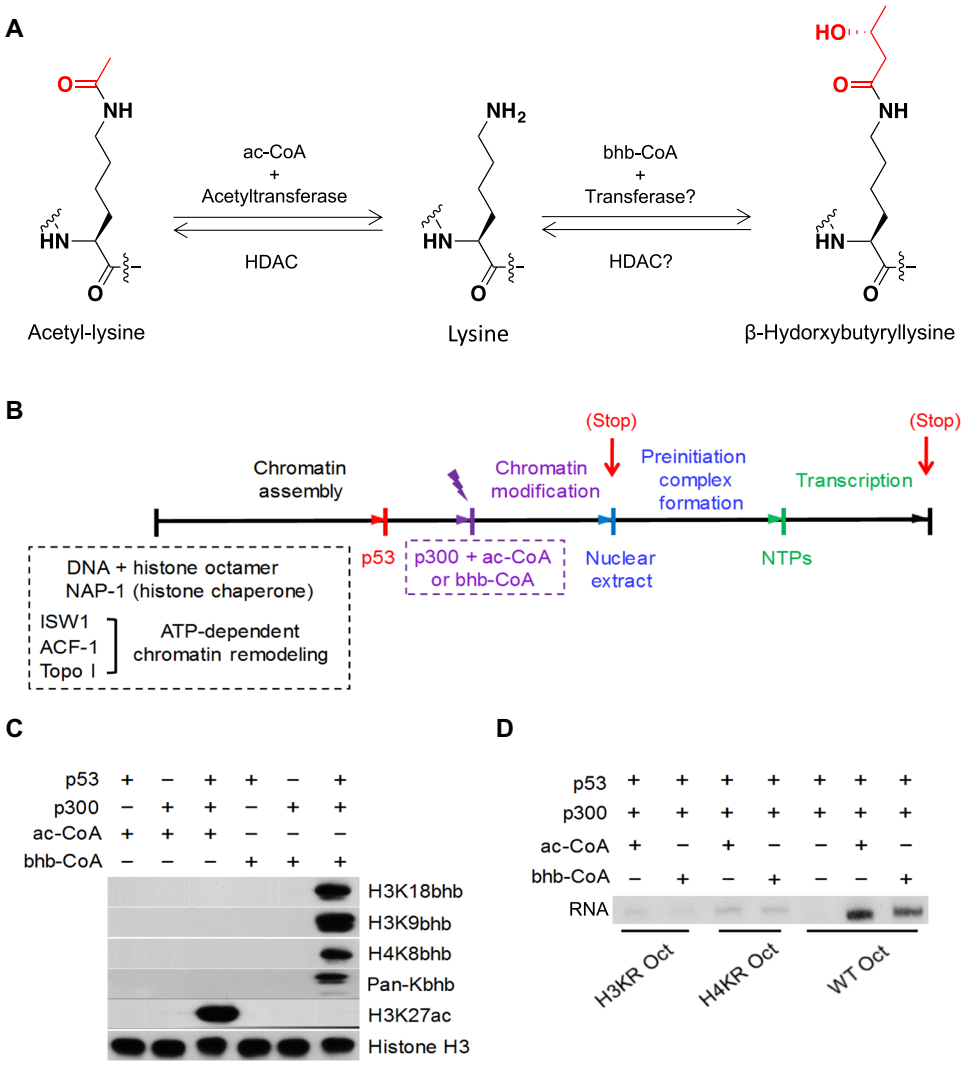

Fig. 1. p53- and p300-dependent histone Kbhb assay on recombinant chromatin templates. (**A**) Illustration of enzymatic reaction for acetyl-lysine and the hypothesized mechanism for β-hydroxybutyryllysine. (**B**) Schematic of the p300-dependent in vitro transcription assay. NTPs, nucleoside triphosphates. (**C**) The histone acyltransferase assay with indicated factors, ac-CoA and bhb-CoA. The Kbhb and Kac levels of histones were analyzed by immunoblotting with indicated antibodies. (**D**) p300-dependent histone Kbhb facilitates active transcription by p53 on recombinant chromatin templates, which can be abolished by histone H3 and H4 K-R mutations. RNA products were visualized by autoradiography. "Oct" represents octamer.

transcription factor p53- and short-chain CoA-dependent histone acylations (Fig. 1B) (*14*, *15*). We first tested whether p300 could catalyze histone Kbhb on recombinant chromatin substrates (Fig. 1C). As a positive control, and as expected, we first showed that histone Kac could be robustly enhanced on core histones in a p300- and ac-CoA–dependent manner, serving as a positive control. Likewise, Kbhb sites on core histone were also elevated in response to addition of p300 and bhb-CoA, indicating that p300 is a histone Kbhb transferase on nucleosomes in vitro.

Next, we examined whether the resulting histone Kbhb can, in turn, mediate in vitro transcription. bhb-CoA could substitute for ac-CoA in facilitating p53-stimulated and p300-dependent in vitro transcription (Fig. 1D). As a further control, and as expected, K-R mutations in either histone H3 or histone H4 abolished the p53-dependent in vitro transcription, regardless of the presence of p300, p53, and ac-CoA (*16*). Together, these two lines of evidence indicate that p300-catalyzed histone Kbhb can directly mediate transcription in vitro.

p300 has histone Kbhb transferase activity in cells

To examine the Kbhb transferase activity of p300 ex vivo, we tested whether p300 could affect the levels of Kbhb on histones in cultured cells. The knockdown of either *p300* or *CREB-binding protein* (*CBP*) slightly, but notably, reduced the levels of Kac and Kbhb on histones (Fig. 2A). To corroborate the knockdown result, we examined Kac and Kbhb levels in *p300* knockout HCT116 cells (Fig. 2B). The results show that levels of multiple histone Kbhb sites were decreased in response to *p300* knockout, with some histone Kbhb sites being more sensitive to *p300* knockout than corresponding Kac sites. Similar results were observed in *p300* knockout mouse embryonic fibroblast (MEF) cells. To confirm Kbhb transferase activity of p300, we treated HCT116 cells with A485, a recently reported potent p300 inhibitor (*17*). As expected, inhibition of p300 by A485 dose-dependently reduced both Kac and Kbhb levels on H3K9, H3K18, and H4K8 (Fig. 2C).

Next, we examined whether other acetyl transferases can catalyze Kbhb reaction. To this end, we overexpressed *p300*, *CBP*, *GCN5*,

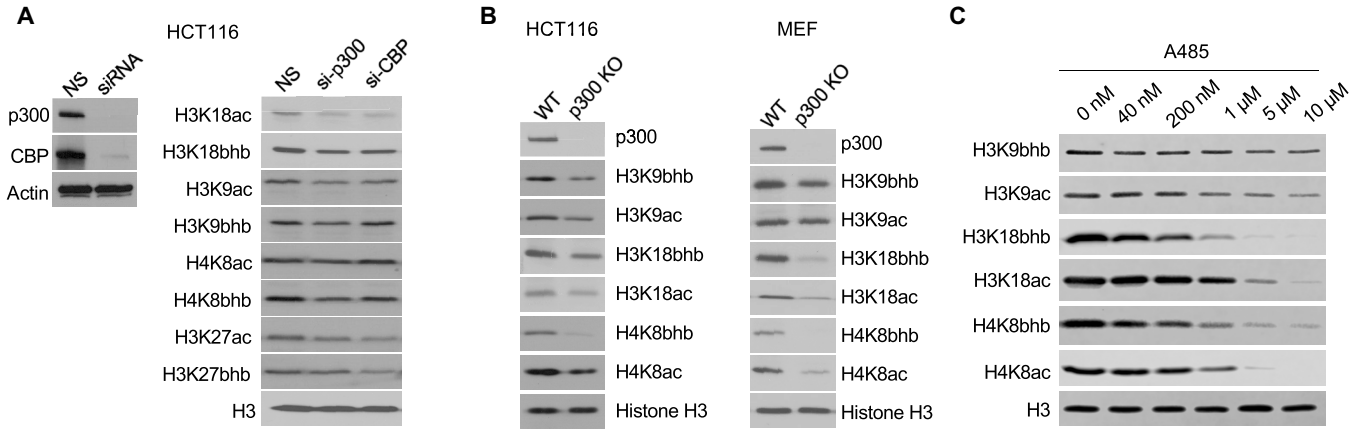

Fig. 2. p300 has histone lysine β-hydroxybutyryltransferase activity in vivo. (**A**) *p300* knockdown by siRNA transfection impairs histone Kbhb in HCT116 cells. Histone Kbhb and Kac levels were analyzed by immunoblotting with indicated antibodies. NS, nonsilencing. (**B**) *p300* knockout (KO) decreases histone Kbhb levels in HCT116 cells. The indicated histone PTMs were analyzed by immunoblotting with indicated antibodies. WT, wild type. (**C**) p300 inhibitor A485 reduces histone Kbhb and Kac levels dose-dependently in HCT116 cells. HCT116 cells were treated with A485 for 24 hours, and the Kbhb and Kac levels of histones were analyzed by immunoblotting with indicated antibodies.

and *p300/CBP-associated factor* (*PCAF*) in 293T cells and determined the dynamics of Kbhb levels by Western blot. The preliminary results showed that overexpression of either *p300* or *CBP* elevated H3K18bhb and H4K8bhb levels, while overexpression of *GCN5* and *PCAF* did not substantially change the levels of H3K18bhb and H4K8bhb (fig. S1). Together, we conclude that p300 is a histone Kbhb transferase both in vitro and ex vivo.

In vitro screening of Kbhb deacylases

Given the fact that some histone deacetylases (HDACs) have acetylation-independent deacylation activities (*18*, *19*), we next asked which HDACs have de–β-hydroxybutyrylation activity. To this end, we first carried out an in vitro assay using 18 recombinant HDACs (including HDAC1 to HDAC11 and SIRT1 to SIRT7) and HeLa cell–derived core histones (Fig. 3A). Our results showed that five HDACs, namely, HDAC1 to HDAC3 and SIRT1 and SIRT2, exhibited notable de-Kbhb activity toward core histones in vitro. The in vitro de-Kbhb activity of the five HDACs was further confirmed by using a Kbhb-containing histone peptide as a substrate followed by a high-performance liquid chromatography (HPLC) assay (Fig. 3B). Together, these data suggest that HDAC1 to HDAC3 and SIRT1 and SIRT2 have de-Kbhb activity in vitro.

HDAC1 and HDAC2 are Kbhb deacylases in cells

We next asked whether the HDACs have deacylation activity of Kbhb ex vivo. First, we tested the ability of HDAC inhibitors to block their deacylation activity. To this end, we dosed cultured HEK293 cells with sodium butyrate (NaBu), trichostatin A (TSA), FK228, and nicotinamide (NAM), with NAM being a class III HDAC inhibitor and the other three reagents being inhibitors for class I and II HDACs. Treatment with the three class I and II HDAC inhibitors, but not with NAM, stimulated both Kac and Kbhb, presumably by blocking HDAC activity (Fig. 4A), suggesting that class I HDACs are the major deacylases for histone Kbhb. In addition, TSA inhibited both Kac and Kbhb in a dose-dependent manner (Fig. 4B). Thus, the deacylation activities of class I/II HDACs were confirmed by the inhibition experiment using HDAC inhibitors.

Next, to determine whether HDAC1 to HDAC3 could catalyze the deacylation of Kbhb in cells, we overexpressed *HDAC1* to *HDAC3* individually in 293T cells. Unexpectedly, we did not observe obvious changes in the histone Kbhb sites that were investigated (fig. S2). A possible reason is that these Kbhb sites are regulated by multiple HDACs, such that the dynamics induced by one HDAC might be compensated by another HDAC with overlapping functions. Given the high deacylase activities of HDAC1 and HDAC2, we next investigated dynamic changes of histone Kbhb in response to HDACs by knocking down both *HDAC1* and *HDAC2*. Notably, the simultaneous knockdown of *HDAC1* and *HDAC2* increased levels of Kbhb in both HEK293 and HeLa cells (Fig. 4C). Combined with the above data, we conclude that HDAC1 and HDAC2 are Kbhb deacylases both in vitro and in cells. In support of this observation, we found that treatment of cells with a selective HDAC1/2/3 inhibitor, MS275, clearly increased multiple Kbhb site signals in a dose-dependent manner (Fig. 4D).

Proteome-wide identification of Kbhb substrates in HEK293 cells

In our previous study, the identified Kbhb sites were limited to histones. However, we now have found that β-hydroxybutyrate treatment increases Kbhb across a wide range of proteins in a dose-dependent manner (fig. S3). In contrast, we did not see an effect on Kac levels for nonhistone proteins among the doses we tested, although β-hydroxybutyrate has been shown to act as an HDAC inhibitor (*20*). This observation is supported by a recent study in which butyrate, but not β-hydroxybutyrate, promotes histone Kac in multiple cell types and in vitro experiment (*21*).

To identify protein substrates bearing Kbhb, we carried out a proteomics screening using an affinity-directed mass spectrometry (MS) method that involves tryptic digestion of extracted proteins, high-pH HPLC fractionation, affinity enrichment of Kbhb peptides with an anti-Kbhb antibody, and, lastly, HPLC-MS/MS analysis and database searching (Fig. 5A). This method led to the identification of 3392 Kbhb sites on 1431 proteins. To improve the reliability of identified sites, the peptides with MaxQuant scores below 40 or localization probabilities below 0.75 were removed. Using such criteria, we identified 3248 unique Kbhb sites on 1397 proteins with high confidence (average site score is 140.33 in MaxQuant).

Next, we experimentally confirmed the identification of Kbhb on two selected nonhistone proteins: non-POU domain-containing

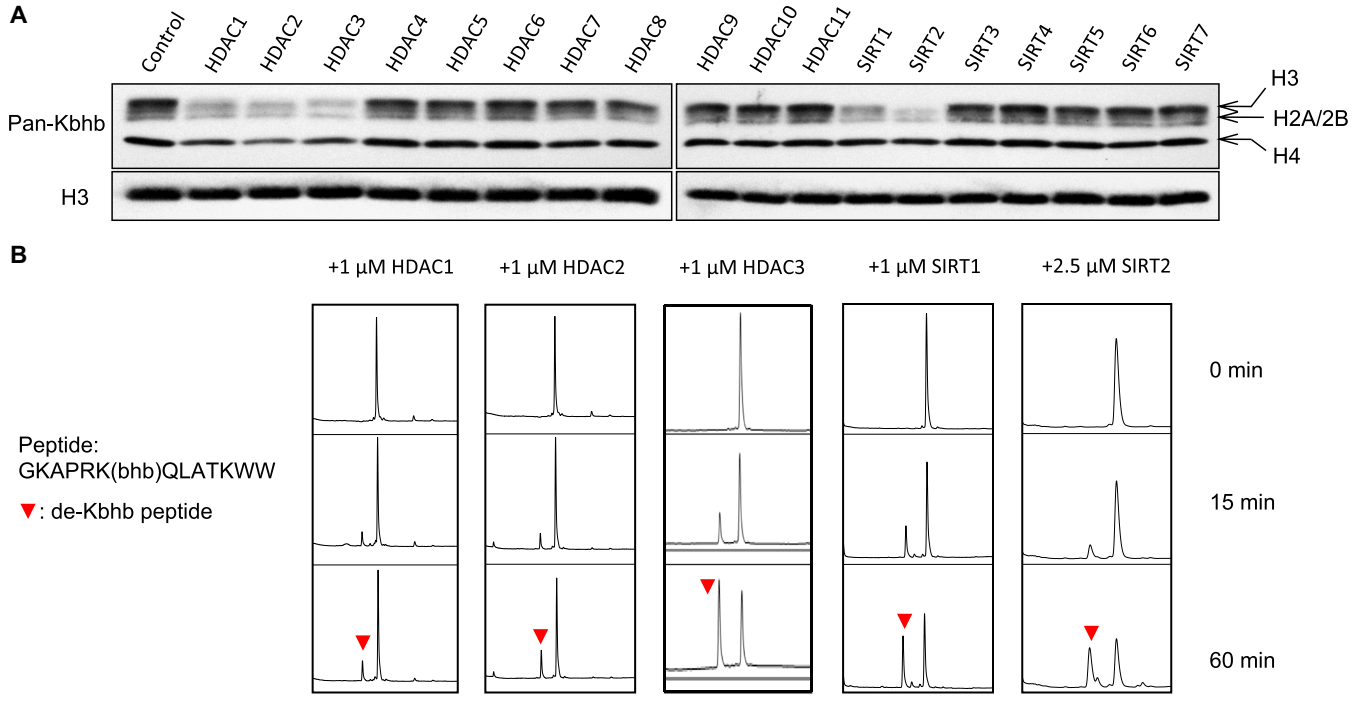

Fig. 3. HDAC1 to HDAC3 and SIRT1 and SIRT2 can remove Kbhb in vitro. (**A**) In vitro screening of HDAC and sirtuins Kbhb deacylase activities. (**B**) Kbhb deacylase activity assay of HDAC1 to HDAC3 and SIRT1 and SIRT2 using Kbhb-containing peptides as substrates.

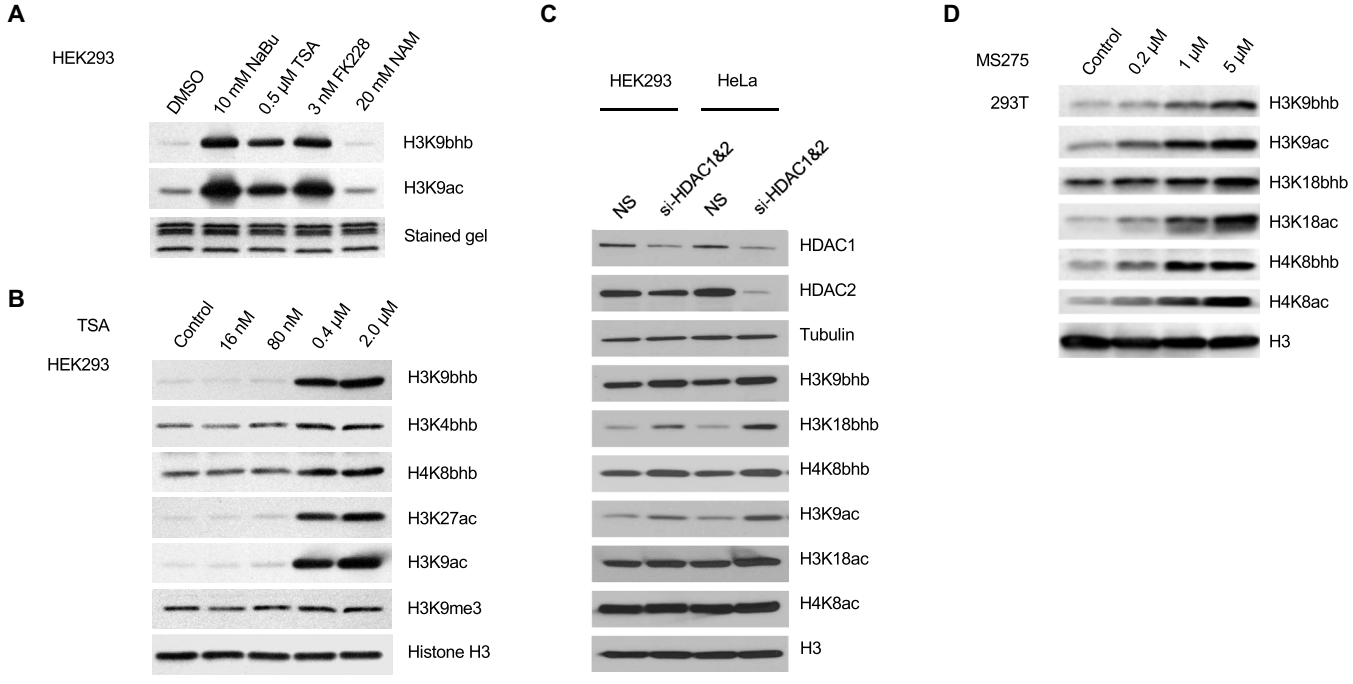

Fig. 4. HDAC1 and HDAC2 remove Kbhb in cells. (**A**) Class I/II HDAC inhibitors (NaBu, TSA, and FK228), but not a class III HDAC inhibitor (NAM), elevate H3K9bhb and H3K9ac levels in HEK293 cells. DMSO, dimethyl sulfoxide. (**B**) TSA treatment increases histone Kbhb levels in HEK293 cells. Cells were treated with TSA at the indicated concentrations for 18 hours, and Kbhb and Kac levels were analyzed by immunoblotting with indicated antibodies. (**C**) Joint knockdown of *HDAC1* and *HDAC2* increases histone Kbhb levels in HEK293 and HeLa cells. Kbhb and Kac levels were detected by immunoblotting using indicated antibodies. Immunoblot of histone H3 was used as loading control. (**D**) An HDAC1/2/3 selective inhibitor, MS275, dose-dependently increases Kbhb and Kac levels in 293T cells. Cells were treated with MS275 for 24 hours, and the Kbhb and Kac levels were analyzed by immunoblotting with the indicated antibodies.

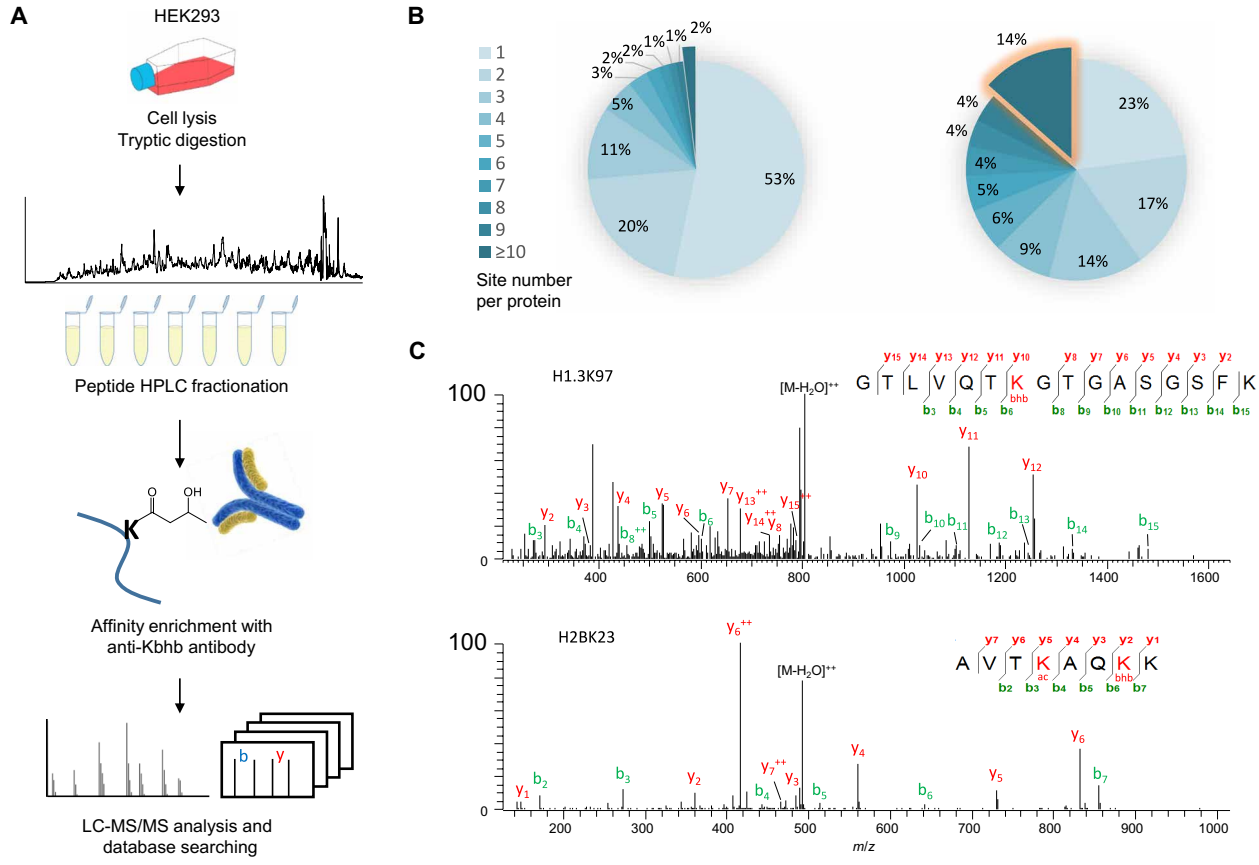

Fig. 5. Systematic profiling of the Kbhb proteome. (**A**) Schematic representation of experimental workflow for the identification of Kbhb-containing protein substrates in HEK293 cells. (**B**) MS/MS spectra of two representative Kbhb peptides derived from HEK293 core histones. (**C**) Distribution of the Kbhb protein (left) and Kbhb sites (right) based on the site number per protein.

octamer-binding protein and nucleophosmin. Flag-tagged target proteins were overexpressed in 293T cells with or without β-hydroxybutyrate treatment. Western blot analysis of the enriched target proteins showed obvious increase of Kbhb levels upon β-hydroxybutyrate treatment (fig. S4).

Analysis of Kbhb sites

In total, we identified 3248 Kbhb sites present in varied distributions across 1397 proteins (table S1). Among these proteins, 53% contain single Kbhb sites, while 2% contain more than 10 Kbhb sites, corresponding to at least 14% of all identified sites (Fig. 5B). We identified 36 histone Kbhb sites, including two previously unknown histone Kbhb sites located at H1K97 and H2BK23, respectively (Fig. 5C and fig. S5).

To identify the Kbhb sites that are likely to be physiologically relevant, we searched the literature for lysine residues that have been reported to be critical for biological functions. We found that some Kbhb sites are located in regions critical for the binding of enzymatic cofactors (table S2). For example, K143 of aurora kinase A and K87 of dual specificity testis-specific protein kinase 2 are important for binding to adenosine 5′-triphosphate (*22*). Similarly, K263 and K268 of ac-CoA acetyltransferase (ACAT1) are necessary for binding to ac-CoA (*23*). The changes in structure and charge state of these lysine residues caused by Kbhb are likely to disrupt cofactor binding to the corresponding enzymes. In addition, 26 Kbhb sites are located at the mutation sites recorded in the UniProt database (table S2). Transcription intermediary factor 1β (TRIM28) is β-hydroxybutyrylated at K779. A previous study showed that the K779R mutation leads to complete abolishment of SUMOylation and transcriptional repression (*24*). Likewise, a K11R mutation in small ubiquitin-related modifier 2 (SUMO2) abolishes the formation of polySUMO chains (*25*). Together, these results suggest that the signaling effects of Kbhb go beyond histone marks by functionally affecting a variety of substrates throughout the proteome.

Sequence preference and functional annotation of the Kbhb proteome

To test for any possible Kbhb motifs in the substrate proteins identified here, we compared the amino acid sequences surrounding Kbhb sites against the human proteome background. We found a notable preference for positive-charged lysines at most positions (−6, −5, −4, −3, 3, 4, 5, and 6), while negative-charged amino acids were underrepresented at the −2 position (Fig. 6A). In addition, alanine was enriched in the +1 and +2 positions. Serine and proline were highly enriched in the −1 and −2 positions, respectively.

We also carried out a cellular compartment analysis to probe the subcellular localizations of the Kbhb proteins in cells (Fig. 6B). We found that Kbhb proteins are more represented in nucleus ($P = 4.37 \times 10^{-236}$), accounting for 78.2% of all proteins. Unlike Ksucc and lysine malonylation (Kma), which occur largely in mitochondria

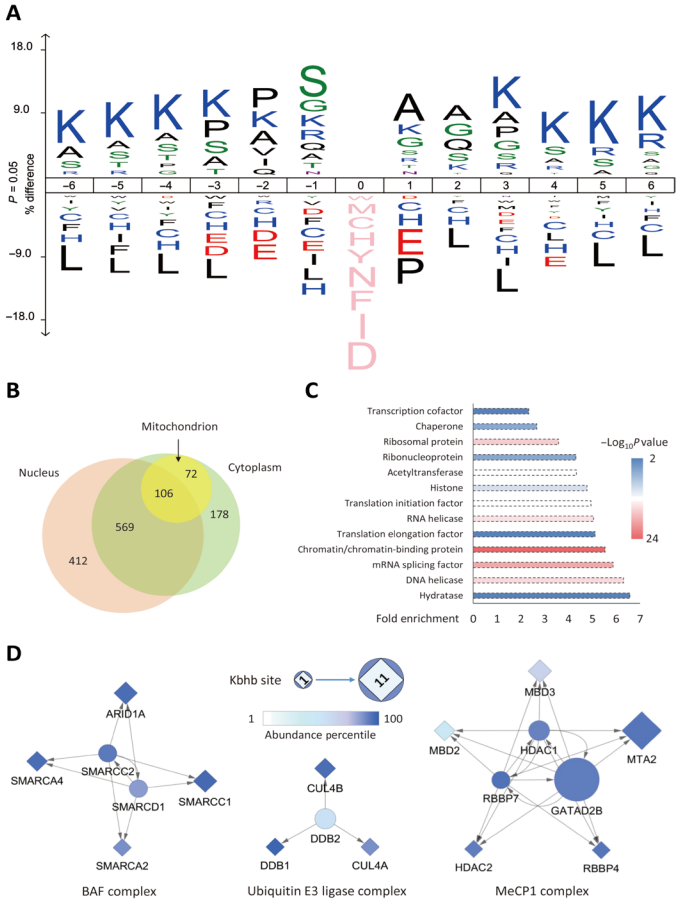

Fig. 6. Characterization of the Kbhb proteome in HEK293 cells. (**A**) Sequence motif logo shows a representative sequence for all Kbhb sites. (**B**) Venn diagram shows the cellular compartment distribution of Kbhb proteins. (**C**) Protein class enrichment of Kbhb proteins. (**D**) Protein complexes enriched in the Kbhb proteome. The color bar depicts the protein abundance percentile in HEK293 cells, and the size stands for the number of Kbhb sites identified in each protein. Circles and squares represent bait and prey nodes, respectively.

(*26*–*28*), only 12.8% Kbhb proteins are located in mitochondrion ($P = 2.65 \times 10^{-5}$), suggesting that Kbhb modifications have regulatory functions largely different from those of Ksucc and Kma.

The Kyoto Encyclopedia of Genes and Genomes (KEGG) pathway enrichment analysis indicated that most Kbhb proteins are involved in spliceosome ($P = 4.84 \times 10^{-43}$), ribosome ($P = 2.16 \times 10^{-13}$), and RNA transport ($P = 2.09 \times 10^{-12}$) functions (table S3). This analysis also showed that DNA repair–related pathways, such as nucleotide excision repair ($P = 3.00 \times 10^{-11}$), mismatch repair ($P = 1.12 \times 10^{-9}$), and base excision repair ($P = 2.78 \times 10^{-7}$), were highly enriched, with 43, 57, and 39% of proteins in these pathways being β-hydroxybutyrylated (table S3). These results also suggest that the Kbhb proteome has a wide distribution of functions that mainly affect the nucleus.

To describe the classification of the Kbhb proteome, we also performed a protein class enrichment analysis (Fig. 6C). Notably, hydratase, DNA helicase, and mRNA splicing factors were highly represented. In addition to these classes, we identified a notable enrichment of chromatin/chromatin-binding proteins ($P = 4.94 \times 10^{-24}$), including a series of bromodomain-containing (BRD2, BRD3, BRD4, BAZ1A, BAZ1B, BAZ2A, BAZ2B, CBP, and BPTF) and epigenetic reader domain–containing (YEATS2) proteins. Some of the members of these protein families are known to specifically recognize histone marks bearing short-chain lysine acylations (*29*, *30*).

Identification of protein complexes for the Kbhb pathway represents a key step toward the description of Kbhb cellular functions. We performed a protein complex enrichment analysis that was facilitated by a manually curated CORUM database (*31*) and the reported protein-protein interaction network (BioPlex 2.0) (Fig. 6D) (*32*). Our analysis showed that BRG-/BRM-associated factor (BAF) ($P = 7.20 \times 10^{-6}$), ubiquitin E3 ligase ($P = 1.05 \times 10^{-4}$), and methyl-CpG–binding domain protein 1 (MeCP1) ($P = 4.19 \times 10^{-8}$) complexes are highly enriched. The BAF complex has been reported to regulate gene expression by remodeling chromatin structure (*33*, *34*). Notably, six of the nine subunits in this complex were β-hydroxybutyrylated, and one of them, transcriptional repressor p66β (GATAD2B), contains 11 Kbhb sites. Similarly, eight of the nine subunits in the MeCP1 complex and four of the five subunits in the ubiquitin E3 ligase complex were β-hydroxybutyrylated. These complexes play important roles in transcription and DNA damage responses, respectively (*35*–*37*). Collectively, these results suggest that Kbhb may also engage in diverse cellular functions, such as chromatin remodeling, transcriptional regulation, and DNA repair.

DISCUSSION

The metabolic importance of β-hydroxybutyrate has been appreciated for many decades. However, its function as a signaling molecule was only discovered recently. It was reported that β-hydroxybutyrate can bind cell surface G protein–coupled receptors (*38*) and influence transmembrane transporters (*39*). β-Hydroxybutyrate is a precursor for histone lysine acylation and can regulate gene expression (*12*). Accordingly, β-hydroxybutyrate can also serve as a signaling molecule in addition to its role as a metabolite.

Functional characterization of the Kbhb pathway demands an understanding of its regulatory elements, including substrate proteins as well as enzymes that can add and remove the modification. In this study, we demonstrate that p300 acts as a Kbhb transferase and has corresponding enzymatic activity both in vitro and in vivo. A previous study showed that this enzyme can bind a family of short-chain acyl-CoAs and catalyze reactions for diverse short-chain lysine acylations (*13*). Using an in vitro reconstituted, chromatin-templated transcription assay, we show that histone Kbhb by p300 can mediate direct transcriptional activation by p53. Our earlier study demonstrates a close correlation of histone H3K9bhb and active gene expression (*12*). These results clearly suggest that histone Kbhb can contribute to chromatin structure and regulation of gene expression. In addition to establishing p300 as the Kbhb writer, we demonstrated that HDAC1 and HDAC2 can serve as erasers of Kbhb. SIRT3 did not decrease global Kbhb level in our in vitro assay, although it recently was reported to show deacylase activity toward Kbhb (*40*). This is not unexpected, because the reported data suggest that SIRT3 predominantly removes (*S*)-Kbhb, while the endogenous Kbhb monitored here is the (*R*)-isoform (*40*). In addition, SIRT3 removes (*R*/*S*)-Kbhb on H3 peptides slowly (*40*). Moreover, the substrates used in our in vitro assay were extracted core histones, such that slight dynamic changes on a few individual sites by SIRT3 may have little influence on the global Kbhb level, especially when compared to HDAC1 to HDAC3. Together, our

study thus identified the major writer and eraser enzymes for the Kbhb pathway.

Emerging evidence suggests that lysine acylations are widely distributed throughout subcellular organelles (*41*). Kbhb was initially identified on histones. However, potential nonhistone protein substrates remained unknown. To address this issue, we performed a comprehensive characterization of Kbhb substrates in HEK293 cells and provide the first global Kbhb proteome dataset, which contains 3248 reliable Kbhb sites on 1397 proteins. Notably, we also identified several previously unidentified histone Kbhb marks, such as H2BK23bhb and H1K97bhb. Moreover, Kbhb proteins were found to be highly enriched in the nucleus, which is quite different from the substrate proteins that bear either Ksucc or Kma and that are prevalent in mitochondria. Consistent with this observation, Kbhb substrates are enriched in proteins associated with diverse nuclear biological processes such as RNA metabolism, chromatin organization, and DNA repair.

Mounting evidence suggests that histones can be modified by diverse enzyme-catalyzed reactions, such as acetylation and methylation (*3*, *42*). In addition, they can also be subjected to spontaneous nonenzymatic reactions, which occur between the nucleophilic side chains of amino acids in proteins and highly electrophilic acyl-CoAs (*1*), e.g., bhb-CoA and ac-CoA. Given that p300 has a strong impact on the levels of histone Kbhb (Fig. 1), we argue that enzyme-catalyzed acylation is the major mechanism for histone Kbhb.

When comparing the Kbhb proteome with reported Kac (*43*), Kcr (*44*), Khib (*43*), and Ksucc proteomes (*45*), we found that only a small part of the modified proteins bear three or more types of PTMs (fig. S6A), and most of the diverse PTMs do not occur at same lysine residues (fig. S6B), suggesting that a large proportion of the PTMs that we investigated have unique functions. In addition, sequence preference analysis of PTM substrate proteins reveals distinct motifs of different PTMs (fig. S6C). KEGG pathway analysis also confirms the unique functions among these acylations (fig. S6D). For example, compared with other types of PTMs, Kac primarily targets proteins involved in RNA biology, while Kcr targets proteins involved in ribosome pathways. On the other hand, Ksucc and Khib are highly enriched in proteins associated with diverse metabolic pathways, whereas Kbhb is associated with DNA repair and spliceosome. These results indicate that different types of PTMs have unique substrate profiles, suggesting differential regulatory mechanisms.

Diverse histone lysine acylations are known to be associated with genetic diseases (*26*, *46*), to contribute to gene expression, and to affect cellular and physiological changes (*18*, *47*, *48*). A fundamental question in this field is how the lysine acylation pathways are differentially regulated. There are several possibilities. One mechanism may be caused by dynamic changes of short-chain CoAs and corresponding short-chain fatty acids. For example, β-hydroxybutyrate can be elevated in a variety of physiological conditions, such as fasting. Recent work by Lu and his colleagues showed that locally generated succinyl-CoA can be used by GCN5 for histone Ksucc (*49*). Thus, local concentration of short-chain fatty acids could be an important factor in influencing particular lysine acylations. In principle, a few possibilities exist: (i) bhb-CoA generation outside of, and then imported into, nuclei; (ii) bhb-CoA generation in situ similar to succinyl-CoA production by the nuclear α–ketoglutarate dehydrogenase complex; and (iii) bhb-CoA is generated from nuclear β-hydroxybutyrate by short-chain CoA synthetase. It will be interesting to examine which mechanism is the driving force for production of nuclear bhb-CoA. Furthermore, we recently showed that p300-dependent Kac and Khib have different substrate profiles, suggesting that the same acyltransferase can produce distinct patterns of lysine acylations (*43*). Third, there may be unique enzymes specific for a lysine acylation. As an example, SIRT5 is a robust eraser for lysine acylations bearing a negative charge but not for lysine acylations with hydrophobic and polar side chains (*50*). Identification of CPT1A as a succinyltransferase also suggests such a possibility (*51*). Last, unique reader proteins may specifically recognize certain PTMs, which, in turn, trigger downstream cellular events. The YEATS domain–containing protein AF9 serves as a good example for this case (*52*). Given the substantial structural difference between Kbhb and other types of PTMs, we speculate the possible existence of reader proteins that can specifically recognize Kbhb and cause downstream alterations in diverse biological processes. It is highly likely that multiple mechanisms could act synergistically for the regulation of diverse lysine acylation pathways.

MATERIALS AND METHODS

Proteins, antibodies, siRNAs, and material

The sequence-specific anti-H3K4bhb (PTM-1258), anti-H3K9bhb (PTM-1250), anti-H3K18bhb (PTM-1252), anti-H3K27bhb (PTM-1293), anti-H4K8bhb (PTM-1253), anti-H3K9ac (PTM-156), anti-H3K18ac (PTM-158), anti-H3K27ac (PTM-160), anti-H4K8ac (PTM-164), and pan anti-Kbhb (PTM-1201) antibodies were purchased from PTM Biolabs Inc. (Chicago, IL). Anti–histone H3 antibody (07-690) was purchased from Millipore (Billerica, MA). Anti-H3K9me3 (ab8898), anti-actin (ab8224), and anti-tubulin (ab6046) antibodies were purchased from Abcam (Cambridge, MA). Anti-p300 antibody (sc-585) and CBP small interfering RNA (siRNA) (sc-29244) were purchased from Santa Cruz Biotechnology (Dallas, TX). Anti-CBP antibody (NB100-91721) was bought from Novus Biologicals (Littleton, CO). HDAC1 to HDAC11 and SIRT1 to SIRT7 enzymes were purchased from BPS Bioscience (San Diego, CA). HDAC1 siRNA, HDAC1 siRNA, and p300 siRNA were purchased from GE Healthcare Dharmacon Inc. (Lafayette, CO). Recombinant human p300 (31124) and p53 (31465) proteins were purchased from Active Motif (Carlsbad, CA).

Other chemicals were obtained from the following suppliers: Sigma-Aldrich (St. Louis, MO): formic acid, trifluoroacetic acid (TFA), Hepes, NH_4HCO_3, trichloroacetic acid (TCA; 6.1 N), dithiothreitol (DTT), iodoacetamide (IAA), EDTA, EGTA, NP-40, sodium β-hydroxybutyrate (Na-bhb), glycerol, urea, acetone, sucrose, ammonium formate, HCl solution (37.3%), Triton X-100, NaBu, TSA, romidepsin (FK228), and NAM. Merck & Co. (Kenilworth, NJ): acetonitrile (ACN; mass spectrometry grade) and water (mass spectrometry grade). Thermo Fisher Scientific (Waltham, MA): Dulbecco's modified Eagle's medium (DMEM) and GlutaMAX. Serum Source International (Charlotte, NC): fetal bovine serum (FBS). C_{18} ZipTips were bought from Millipore (Billerica, MA).

Cell culture and protein preparation

HEK293 [American Type Culture Collection (ATCC) CRL-1573], HEK293T (ATCC CRL-11268), HeLa (ATCC CCL-2), HCT116 (ATCC CCL-247), and MEF (ATCC SCRC-1040) cells were cultured in DMEM containing 10% FBS, 1% GlutaMAX, and 5% CO_2. For proteomics analysis, HEK293 cells were treated with 10 mM Na-bhb for 24 hours. Then, the collected cells were washed twice

with ice-cold phosphate-buffered saline and suspended in a lysis buffer (8 M urea, 2 mM EDTA, 3 μM TSA, 50 mM NAM, 5 mM DTT, and 1% Protease Inhibitor Cocktail III), followed by ultrasonication on ice. After centrifugation at 16,000*g* at 4°C for 15 min, the supernatants were collected and processed with TCA precipitation. The protein concentration was determined by Bradford assay.

Histone proteins were extracted using a previously published method (*53*). Briefly, HCT116, MEF, HEK293, and HeLa cells were suspended in cold extraction buffer [10 mM Hepes (pH 8.0), 10 mM KCl, 1.5 mM $MgCl_2$, 0.34 M sucrose, and 0.1% Triton X-100] at 4°C for 30 min. After centrifugation, the pellets were resuspended in 300 μl of no-salt buffer (3 mM EDTA and 0.2 mM EGTA) and incubated on a rotator at 4°C for 30 min. After washing two times, the pellets were extracted with 0.2 M H_2SO_4 at 4°C overnight. The suspensions were centrifuged at 16,000*g* for 15 min at 4°C. Then, the histone-containing supernatants were precipitated by slowly adding 20% (v/v) TCA. The precipitated histone pellets were washed twice with cold acetone and dried at 4°C, followed with protein concentration determination by Bradford assay.

Protein digestion

The proteins extracted from HEK293 cells were subjected to in-solution tryptic digestion with minor modifications of a previously reported method (*54*). Briefly, the proteins were reduced in 20 mM DTT at 37°C for 1.5 hours, and the products were alkylated in 40 mM IAA at room temperature in the dark for 30 min. After that, trypsin was added into the solution (trypsin:protein = 1:50, w/w), and the mixtures were incubated at 37°C for 12 hours before peptide fractionation.

Peptide fractionation and immunoaffinity enrichment

We used HPLC buffer A (10 mM ammonium formate in water, pH 7.8) and HPLC buffer B (10 mM ammonium formate in 90% acetonitrile and 10% water, pH 7.8) for high-pH reverse-phase fractionation of peptides. The reverse-phase Agilent 300 Extend C18 column [5-μm particles, 4.6 mm inner diameter, and 250 mm length] was equilibrated with 2% HPLC buffer B. The peptide mixture of interest in HPLC buffer A was loaded onto the HPLC column and eluted with linear gradient of 2 to 30% HPLC buffer B in 60 min, 30 to 90% buffer B in 15 min, and 90% buffer B in 15 min. Eighty-one fractions were collected and combined into 27 final fractions over equal time intervals, followed by lyophilization using SpeedVac.

Enrichment of Kbhb peptides from different fractions by immunoprecipitation with pan anti-Kbhb antibody was carried out as described previously (*54*). Briefly, the peptides were first dissolved in NETN buffer [100 mM NaCl, 50 mM tris-HCl, 1 mM EDTA, and 0.5% NP-40 (pH 8.0)] and incubated with pan anti-Kbhb beads at 4°C overnight. Then, the beads were washed three times with NETN buffer and twice with ddH_2O. The combined peptides were eluted with 0.1% (v/v) TFA. The isolated Kbhb peptides were dried in SpeedVac.

HPLC-MS/MS analysis and database searching

The resulting peptide samples were dissolved in 2.5 μl of buffer A (0.1% formic acid in water, v/v) and loaded onto a homemade capillary column (10 cm length with 75 μm ID) packed with Jupiter C12 resin (4-μm particle size, 90-Å pore size; Phenomenex) connected to an EASY-nLC 1000 HPLC system (Thermo Fisher Scientific, Odense, Denmark). Peptides were eluted with a 2-hour gradient of 8 to 28% buffer B (0.1% formic acid in 90% ACN) in 85 min, 28 to 90% buffer B in 12.5 min, and 90% buffer B in 22.5 min at a flow rate of 200 nl min^{-1}. The Linear Trap Quadrupole Orbitrap Velos MS was operated in positive ion data-dependent mode, and the 20 most intense ions were subjected to collision-induced dissociation fragmentation with the normalized collision energy at 35%. The MS1 scan was performed at a resolution of 30,000 from *m*/*z* (mass/charge ratio) 350 to 1800 (automatic gain control value, 1×10^6; maximum injection time, 30 ms). The MS/MS scans were performed in ion trap. The repeat duration for the data-dependent scan was 5 s, the repeat count was 2, and the exclusion duration was set at 90 s. Following procedures previously described (*55*), the unassigned ions or those with a charge of +1 and >+5 were rejected. One microscan was acquired for each MS and MS/MS scan. A lock mass correction was also appended using a background ion (*m*/*z* 445.12002).

The raw data were uploaded into MaxQuant (version 1.3.0.5) and were searched against the UniProtKB human complete proteome sequence database (release April 2017). The reverse sequences were appended for a false discovery rate (FDR) evaluation. The mass tolerances were set at 10 parts per million for the parent ions and at 0.5 Da for the fragments. The peptides were searched using tryptic cleavage constraints, and a maximum of two missed cleavages were allowed. The minimal peptide length was seven amino acids. Carbamidomethylation (C, +57.0215 Da) was used as the fixed modification. Oxidation (M, +15.9949 Da), acetylation (K, +42.0106 Da), and β-hydroxybutyrylation (K, +86.0368 Da) were included as variable modifications. Results were further filtered by a 1% FDR at protein, peptide, and site levels. We also removed the peptides with MaxQuant score below 40 or site localization probability below 0.75.

Western blot

Protein extracts (2 to 4 μg of histone or 20 μg of whole-cell lysate) were separated in SDS–polyacrylamide gel electrophoresis and then transferred to polyvinylidene difluoride membrane. The membrane was blocked in 3% bovine serum albumin in TBST [20 mM tris (pH 7.6), 150 mM NaCl, and 0.1% Tween 20] for 1 hour at room temperature. The membranes were then incubated overnight at 4°C in primary solutions. The resulting membranes were washed in TBST and incubated in horseradish peroxidase–conjugated secondary antibody solutions for 1 hour at room temperature. The membranes were washed again in TBST before detecting signal using enhanced chemiluminescence system.

siRNA transfection

Transfection of siRNAs was performed according to the manufacturer's instructions. Briefly, cells were trypsinized and plated in six-well dishes at 2.5×10^4 cells per well for 12 to 16 hours before transfection. Cationic lipid complexes, prepared by incubating 200 pmol of the indicated siRNA with 2 μl of DharmaFECT (Dharmacon) in 100 μl of DMEM for 20 min, were added to the wells in a final volume of 1 ml. After 12 hours, cells were passaged and harvested at 48 hours for Kbhb immunoblot.

In vitro Kac and Kbhb assay

In each band, 250 ng of p53 and/or p300 proteins, 2.5 μg of histone H3 or H4 protein, and 10 μM ac-CoA and/or bhb-CoA were added in reaction buffer [50 mM tris-HCI (pH 8.0), 10% glycerol, 10 mM butyric acid, 0.1 mM EDTA, 1 mM DTT, and 1 mM phenylmethylsulfonyl fluoride]. The mixtures were incubated at 30°C for 1 hour, followed with detection of the levels of Kac and Kbhb by Western blot.

In vitro transcription assay

The materials and method used for in vitro transcription assays were described previously (*14*), except that bhb-CoA was used as the high-energy acyl donor in addition to ac-CoA. Histone modifications were detected by immunoblot, and the in vitro transcription products were detected by autoradiography as previously described (*14*).

In vitro de-Kbhb assay

The in vitro de-Kbhb assay was performed based on our previous report (*15*) using 18 recombinant HDAC candidates.

Bioinformatics analyses

Sequence preference motif was generated by iceLogo using the human proteome as the background (*56*). Gene ontology analysis was performed using Bonferroni correction for multiple testing in PANTHER (version 12.0) (*57*). The identified Kbhb sites were matched with the recorded binding and mutation sites extracted from the UniProt database (www.uniprot.org). The KEGG pathway enrichment analysis was carried out with the help of GOstats package along with a hypergeometric test in R (*58*). Protein complexes were enriched on the basis of the CORUM mammalian protein complex database (*31*) using hypergeometric test. The protein complexes of interest were further described by BioPlex 2.0 (*32*, *59*) based on the known protein-protein interaction network and finally visualized in Cytoscape (version 3.3.0).

SUPPLEMENTARY MATERIALS

Supplementary material for this article is available at http://advances.sciencemag.org/cgi/content/full/7/9/eabe2771/DC1

View/request a protocol for this paper from *Bio-protocol*.

REFERENCES AND NOTES

1. K. L. Diehl, T. W. Muir, Chromatin as a key consumer in the metabolite economy. *Nat. Chem. Biol.* **16**, 620–629 (2020).
2. R. E. Moellering, B. F. Cravatt, Functional lysine modification by an intrinsically reactive primary glycolytic metabolite. *Science* **341**, 549–553 (2013).
3. B. M. Dancy, P. A. Cole, Protein lysine acetylation by p300/CBP. *Chem. Rev.* **115**, 2419–2452 (2015).
4. H. Jiang, X. Zhang, X. Chen, P. Aramsangtienchai, Z. Tong, H. Lin, Protein lipidation: Occurrence, mechanisms, biological functions, and enabling technologies. *Chem. Rev.* **118**, 919–988 (2018).
5. M. Luo, Chemical and biochemical perspectives of protein lysine methylation. *Chem. Rev.* **118**, 6656–6705 (2018).
6. L. Laffel, Ketone bodies: A review of physiology, pathophysiology and application of monitoring to diabetes. *Diabetes Metab. Res. Rev.* **15**, 412–426 (1999).
7. A. M. Robinson, D. H. Williamson, Physiological roles of ketone bodies as substrates and signals in mammalian tissues. *Physiol. Rev.* **60**, 143–187 (1980).
8. J. H. Koeslag, T. D. Noakes, A. W. Sloan, Post-exercise ketosis. *J. Physiol.* **301**, 79–90 (1980).
9. M. Sheikh-Ali, B. S. Karon, A. Basu, Y. C. Kudva, L. A. Muller, J. Xu, W. F. Schwenk, J. M. Miles, Can serum β-hydroxybutyrate be used to diagnose diabetic ketoacidosis? *Diabetes Care* **31**, 643–647 (2008).
10. M. A. McNally, A. L. Hartman, Ketone bodies in epilepsy. *J. Neurochem.* **121**, 28–35 (2012).
11. B. G. Allen, S. K. Bhatia, C. M. Anderson, J. M. Eichenberger-Gilmore, Z. A. Sibenaller, K. A. Mapuskar, J. D. Schoenfeld, J. M. Buatti, D. R. Spitz, M. A. Fath, Ketogenic diets as an adjuvant cancer therapy: History and potential mechanism. *Redox Biol.* **2**, 963–970 (2014).
12. Z. Xie, D. Zhang, D. Chung, Z. Tang, H. Huang, L. Dai, S. Qi, J. Li, G. Colak, Y. Chen, C. Xia, C. Peng, H. Ruan, M. Kirkey, D. Wang, L. M. Jensen, O. K. Kwon, S. Lee, S. D. Pletcher, M. Tan, D. B. Lombard, K. P. White, H. Zhao, J. Li, R. G. Roeder, X. Yang, Y. Zhao, Metabolic regulation of gene expression by histone lysine β-hydroxybutyrylation. *Mol. Cell* **62**, 194–206 (2016).
13. Z. Kaczmarska, E. Ortega, A. Goudarzi, H. Huang, S. Kim, J. A. Márquez, Y. Zhao, S. Khochbin, D. Panne, Structure of p300 in complex with acyl-CoA variants. *Nat. Chem. Biol.* **13**, 21–29 (2017).
14. Z. Tang, W.-Y. Chen, M. Shimada, U. T. T. Nguyen, J. Kim, X.-J. Sun, T. Sengoku, R. K. McGinty, J. P. Fernandez, T. W. Muir, R. G. Roeder, SET1 and p300 act synergistically, through coupled histone modifications, in transcriptional activation by p53. *Cell* **154**, 297–310 (2013).
15. H. Huang, Z. Luo, S. Qi, J. Huang, P. Xu, X. Wang, L. Gao, F. Li, J. Wang, W. Zhao, W. Gu, Z. Chen, L. Dai, J. Dai, Y. Zhao, Landscape of the regulatory elements for lysine 2-hydroxyisobutyrylation pathway. *Cell Res.* **28**, 111–125 (2018).
16. W. An, V. B. Palhan, M. A. Karymov, S. H. Leuba, R. G. Roeder, Selective requirements for histone H3 and H4 N termini in p300-dependent transcriptional activation from chromatin. *Mol. Cell* **9**, 811–821 (2002).
17. L. M. Lasko, C. G. Jakob, R. P. Edalji, W. Qiu, D. Montgomery, E. L. Digiammarino, T. M. Hansen, R. M. Risi, R. Frey, V. Manaves, B. Shaw, M. Algire, P. Hessler, L. T. Lam, T. Uziel, E. Faivre, D. Ferguson, F. G. Buchanan, R. L. Martin, M. Torrent, G. G. Chiang, K. Karukurichi, J. W. Langston, B. T. Weinert, C. Choudhary, P. de Vries, J. H. Van Drie, D. McElligott, E. Kesicki, R. Marmorstein, C. Sun, P. A. Cole, S. H. Rosenberg, M. R. Michaelides, A. Lai, K. D. Bromberg, Discovery of a selective catalytic p300/CBP inhibitor that targets lineage-specific tumours. *Nature* **550**, 128–132 (2017).
18. B. R. Sabari, D. Zhang, C. D. Allis, Y. Zhao, Metabolic regulation of gene expression through histone acylations. *Nat. Rev. Mol. Cell Biol.* **18**, 90–101 (2017).
19. P. Bheda, H. Jing, C. Wolberger, H. Lin, The substrate specificity of sirtuins. *Annu. Rev. Biochem.* **85**, 405–429 (2016).
20. T. Shimazu, M. D. Hirschey, J. Newman, W. He, K. Shirakawa, N. Le Moan, C. A. Grueter, H. Lim, L. R. Saunders, R. D. Stevens, C. B. Newgard, R. V. Farese Jr., R. de Cabo, S. Ulrich, K. Akassoglou, E. Verdin, Suppression of oxidative stress by β-hydroxybutyrate, an endogenous histone deacetylase inhibitor. *Science* **339**, 211–214 (2013).
21. S. Chriett, A. Dąbek, M. Wojtala, H. Vidal, A. Balcerczyk, L. Pirola, Prominent action of butyrate over β-hydroxybutyrate as histone deacetylase inhibitor, transcriptional modulator and anti-inflammatory molecule. *Sci. Rep.* **9**, 742 (2019).
22. M. W. Richards, S. G. Burgess, E. Poon, A. Carstensen, M. Eilers, L. Chesler, R. Bayliss, Structural basis of N-Myc binding by Aurora-A and its destabilization by kinase inhibitors. *Proc. Natl. Acad. Sci. U.S.A.* **113**, 13726–13731 (2016).
23. A. M. Haapalainen, G. Meriläinen, P. L. Pirilä, N. Kondo, T. Fukao, R. K. Wierenga, Crystallographic and kinetic studies of human mitochondrial acetoacetyl-CoA thiolase: The importance of potassium and chloride ions for its structure and function. *Biochemistry* **46**, 4305–4321 (2007).
24. A. V. Ivanov, H. Peng, V. Yurchenko, K. L. Yap, D. G. Negorev, D. C. Schultz, E. Psulkowski, W. J. Fredericks, D. E. White, G. G. Maul, M. J. Sadofsky, M.-M. Zhou, F. J. Rauscher III, PHD domain-mediated E3 ligase activity directs intramolecular sumoylation of an adjacent bromodomain required for gene silencing. *Mol. Cell* **28**, 823–837 (2007).
25. M. H. Tatham, E. Jaffray, O. A. Vaughan, J. M. Desterro, C. H. Botting, J. H. Naismith, R. T. Hay, Polymeric chains of SUMO-2 and SUMO-3 are conjugated to protein substrates by SAE1/SAE2 and Ubc9. *J. Biol. Chem.* **276**, 35368–35374 (2001).
26. G. Colak, O. Pougovkina, L. Dai, M. Tan, H. Te Brinke, H. Huang, Z. Cheng, J. Park, X. Wan, X. Liu, W. W. Yue, R. J. A. Wanders, J. W. Locasale, D. B. Lombard, V. C. J. de Boer, Y. Zhao, Proteomic and biochemical studies of lysine malonylation suggest its malonic aciduria-associated regulatory role in mitochondrial function and fatty acid oxidation. *Mol. Cell. Proteomics* **14**, 3056–3071 (2015).
27. X. Li, X. Hu, Y. Wan, G. Xie, X. Li, D. Chen, Z. Cheng, X. Yi, S. Liang, F. Tan, Systematic identification of the lysine succinylation in the protozoan parasite *Toxoplasma gondii*. *J. Proteome Res.* **13**, 6087–6095 (2014).
28. Y. Nishida, M. J. Rardin, C. Carrico, W. He, A. K. Sahu, P. Gut, R. Najjar, M. Fitch, M. Hellerstein, B. W. Gibson, E. Verdin, SIRT5 regulates both cytosolic and mitochondrial protein malonylation with glycolysis as a major target. *Mol. Cell* **59**, 321–332 (2015).
29. C. Dhalluin, J. E. Carlson, L. Zeng, C. He, A. K. Aggarwal, M.-M. Zhou, Structure and ligand of a histone acetyltransferase bromodomain. *Nature* **399**, 491–496 (1999).
30. T. Kanno, Y. Kanno, R. M. Siegel, M. K. Jang, M. J. Lenardo, K. Ozato, Selective recognition of acetylated histones by bromodomain proteins visualized in living cells. *Mol. Cell* **13**, 33–43 (2004).
31. A. Ruepp, B. Waegele, M. Lechner, B. Brauner, I. Dunger-Kaltenbach, G. Fobo, G. Frishman, C. Montrone, H.-W. Mewes, CORUM: The comprehensive resource of mammalian protein complexes—2009. *Nucleic Acids Res.* **38**, D497–D501 (2009).
32. E. L. Huttlin, R. J. Bruckner, J. A. Paulo, J. R. Cannon, L. Ting, K. Baltier, G. Colby, F. Gebreab, M. P. Gygi, H. Parzen, J. Szpyt, S. Tam, G. Zarraga, L. Pontano-Vaites, S. Swarup, A. E. White, D. K. Schweppe, R. Rad, B. K. Erickson, R. A. Obar, K. G. Guruharsha, K. Li, S. Artavanis-Tsakonas, S. P. Gygi, J. W. Harper, Architecture of the human interactome defines protein communities and disease networks. *Nature* **545**, 505–509 (2017).
33. R. Liu, H. Liu, X. Chen, M. Kirby, P. O. Brown, K. Zhao, Regulation of CSF1 promoter by the SWI/SNF-like BAF complex. *Cell* **106**, 309–318 (2001).
34. K. Zhao, W. Wang, O. J. Rando, Y. Xue, K. Swiderek, A. Kuo, G. R. Crabtree, Rapid and phosphoinositol-dependent binding of the SWI/SNF-like BAF complex to chromatin after T lymphocyte receptor signaling. *Cell* **95**, 625–636 (1998).

35. H.-H. Ng, Y. Zhang, B. Hendrich, C. A. Johnson, B. M. Turner, H. Erdjument-Bromage, P. Tempst, D. Reinberg, A. Bird, MBD2 is a transcriptional repressor belonging to the MeCP1 histone deacetylase complex. *Nat. Genet.* **23**, 58–61 (1999).
36. Q. Feng, Y. Zhang, The MeCP1 complex represses transcription through preferential binding, remodeling, and deacetylating methylated nucleosomes. *Genes Dev.* **15**, 827–832 (2001).
37. H. Wang, L. Zhai, J. Xu, H.-Y. Joo, S. Jackson, H. Erdjument-Bromage, P. Tempst, Y. Xiong, Y. Zhang, Histone H3 and H4 ubiquitylation by the CUL4-DDB-ROC1 ubiquitin ligase facilitates cellular response to DNA damage. *Mol. Cell* **22**, 383–394 (2006).
38. Y.-J. Won, V. B. Lu, H. L. Puhl III, S. R. Ikeda, β-Hydroxybutyrate modulates N-type calcium channels in rat sympathetic neurons by acting as an agonist for the G-protein-coupled receptor FFA3. *J. Neurosci.* **33**, 19314–19325 (2013).
39. S. F. Sleiman, J. Henry, R. Al-Haddad, L. El Hayek, E. A. Haidar, T. Stringer, D. Ulja, S. S. Karuppagounder, E. B. Holson, R. R. Ratan, Exercise promotes the expression of brain derived neurotrophic factor (BDNF) through the action of the ketone body β-hydroxybutyrate. *eLife* **5**, e15092 (2016).
40. X. Zhang, R. Cao, J. Niu, S. Yang, H. Ma, S. Zhao, H. Li, Molecular basis for hierarchical histone de-β-hydroxybutyrylation by SIRT3. *Cell Discov.* **5**, 35 (2019).
41. C. Choudhary, B. T. Weinert, Y. Nishida, E. Verdin, M. Mann, The growing landscape of lysine acetylation links metabolism and cell signalling. *Nat. Rev. Mol. Cell Biol.* **15**, 536–550 (2014).
42. S. Y. Roth, J. M. Denu, C. D. Allis, Histone acetyltransferases. *Annu. Rev. Biochem.* **70**, 81–120 (2001).
43. H. Huang, S. Tang, M. Ji, Z. Tang, M. Shimada, X. Liu, S. Qi, J. W. Locasale, R. G. Roeder, Y. Zhao, X. Li, p300-mediated lysine 2-hydroxyisobutyrylation regulates glycolysis. *Mol. Cell* **70**, 663–678.e6 (2018).
44. H. Huang, D.-L. Wang, Y. Zhao, Quantitative crotonylome analysis expands the roles of p300 in the regulation of lysine crotonylation pathway. *Proteomics* **18**, e1700230 (2018).
45. J. Park, Y. Chen, D. X. Tishkoff, C. Peng, M. Tan, L. Dai, Z. Xie, Y. Zhang, B. M. M. Zwaans, M. E. Skinner, D. B. Lombard, Y. Zhao, SIRT5-mediated lysine desuccinylation impacts diverse metabolic pathways. *Mol. Cell* **50**, 919–930 (2013).
46. O. Pougovkina, H. te Brinke, R. J. A. Wanders, S. M. Houten, V. C. J. de Boer, Aberrant protein acylation is a common observation in inborn errors of acyl-CoA metabolism. *J. Inherit. Metab. Dis.* **37**, 709–714 (2014).
47. X. Li, G. Egervari, Y. Wang, S. L. Berger, Z. Lu, Regulation of chromatin and gene expression by metabolic enzymes and metabolites. *Nat. Rev. Mol. Cell Biol.* **19**, 563–578 (2018).
48. S. Trefely, C. D. Lovell, N. W. Snyder, K. E. Wellen, Compartmentalised acyl-CoA metabolism and roles in chromatin regulation. *Mol. Metab.* **38**, 100941 (2020).
49. Y. Wang, Y. R. Guo, K. Liu, Z. Yin, R. Liu, Y. Xia, L. Tan, P. Yang, J.-H. Lee, X.-j. Li, D. Hawke, Y. Zheng, X. Qian, J. Lyu, J. He, D. Xing, Y. J. Tao, Z. Lu, KAT2A coupled with the α-KGDH complex acts as a histone H3 succinyltransferase. *Nature* **552**, 273–277 (2017).
50. M. D. Hirschey, Y. Zhao, Metabolic regulation by lysine malonylation, succinylation, and glutarylation. *Mol. Cell. Proteomics* **14**, 2308–2315 (2015).
51. K. Kurmi, S. Hitosugi, E. K. Wiese, F. Boakye-Agyeman, W. I. Gonsalves, Z. Lou, L. M. Karnitz, M. P. Goetz, T. Hitosugi, Carnitine palmitoyltransferase 1A has a lysine succinyltransferase activity. *Cell Rep.* **22**, 1365–1373 (2018).
52. Y. Li, B. R. Sabari, T. Panchenko, H. Wen, D. Zhao, H. Guan, L. Wan, H. Huang, Z. Tang, Y. Zhao, R. G. Roeder, X. Shi, C. D. Allis, H. Li, Molecular coupling of histone crotonylation and active transcription by AF9 YEATS domain. *Mol. Cell* **62**, 181–193 (2016).
53. D. Shechter, H. L. Dormann, C. D. Allis, S. B. Hake, Extraction, purification and analysis of histones. *Nat. Protoc.* **2**, 1445–1457 (2007).
54. M. Tan, H. Luo, S. Lee, F. Jin, J. S. Yang, E. Montellier, T. Buchou, Z. Cheng, S. Rousseaux, N. Rajagopal, Z. Lu, Z. Ye, Q. Zhu, J. Wysocka, Y. Ye, S. Khochbin, B. Ren, Y. Zhao, Identification of 67 histone marks and histone lysine crotonylation as a new type of histone modification. *Cell* **146**, 1016–1028 (2011).
55. Y. Weng, Z. Sui, Y. Shan, H. Jiang, Y. Zhou, X. Zhu, Z. Liang, L. Zhang, Y. Zhang, In-depth proteomic quantification of cell secretome in serum-containing conditioned medium. *Anal. Chem.* **88**, 4971–4978 (2016).
56. N. Colaert, K. Helsens, L. Martens, J. Vandekerckhove, K. Gevaert, Improved visualization of protein consensus sequences by iceLogo. *Nat. Methods* **6**, 786–787 (2009).
57. H. Mi, S. Poudel, A. Muruganujan, J. T. Casagrande, P. D. Thomas, PANTHER version 10: Expanded protein families and functions, and analysis tools. *Nucleic Acids Res.* **44**, D336–D342 (2016).
58. S. Falcon, R. Gentleman, Using GOstats to test gene lists for GO term association. *Bioinformatics* **23**, 257–258 (2006).
59. D. K. Schweppe, E. L. Huttlin, J. W. Harper, S. P. Gygi, BioPlex Display: An interactive suite for large-scale, AP-MS protein-protein interaction data. *J. Proteome Res.* **17**, 722–726 (2017).

Acknowledgments

Funding: This work was supported by the University of Chicago; the Nancy and Leonard Florsheim Family Fund (Y.Z.); and NIH grants GM135504 and DK118266 (Y.Z.), NIH GM62437 (P.A.C.), and NIH DK071900 and CA129325 (R.G.R.). We also acknowledge the National Natural Science Foundation of China 81973164 (H.H.) and Shanghai Pujiang Program 19PJ1411200 (H.H.). **Author contributions:** Y.Z. and H.H conceived the project and developed the research strategy. H.H. performed the proteomics study. H.H. and Y.W. analyzed the proteomics data. H.H., D.Z., C.Y., S.Q., and C.P. performed most of the biology experiments. Z.T. and R.G.R. were involved in the in vitro chromatin-based transcription experiments. P.A.C. was involved in the p300 inhibition experiments. H.H., Y.W., K.D., and Y.Z. wrote the manuscript with input from all authors. **Competing interests:** Y.Z. is a founder, board member, equity holder, advisor to, and inventor on patents licensed to PTM Biolabs Inc. (Hangzhou, China and Chicago, IL) and Maponos Therapeutics Inc. (Chicago, IL). P.A.C. is a cofounder and equity holder for Acylin Therapeutics Inc. (Seattle, WA) and a paid advisor for Acylin Therapeutics Inc. and AbbVie Inc. (Chicago, IL). The authors declare that they have no other competing interests. **Data and materials availability:** All data needed to evaluate the conclusions in the paper are present in the paper and/or the Supplementary Materials. Additional data related to this paper may be requested from the authors. The mass spectrometry proteomics data have been deposited to the ProteomeXchange Consortium via the PRIDE partner repository with the dataset identifier PXD012328.

Submitted 11 August 2020
Accepted 12 January 2021
Published 24 February 2021
10.1126/sciadv.abe2771

Citation: H. Huang, D. Zhang, Y. Weng, K. Delaney, Z. Tang, C. Yan, S. Qi, C. Peng, P. A. Cole, R. G. Roeder, Y. Zhao, The regulatory enzymes and protein substrates for the lysine β-hydroxybutyrylation pathway. *Sci. Adv.* **7**, eabe2771 (2021).